Journal of Geophysical Research: Biogeosciences

RESEARCH ARTICLE
10.1002/2017JG004040

Forecasting Responses of a Northern Peatland Carbon Cycle to Elevated CO_2 and a Gradient of Experimental Warming

Jiang Jiang[1], Yuanyuan Huang[2], Shuang Ma[3], Mark Stacy[4], Zheng Shi[2], Daniel M. Ricciuto[5], Paul J. Hanson[5], and Yiqi Luo[3,6]

[1]Key Laboratory of Soil and Water Conservation and Ecological Restoration in Jiangsu Province, Collaborative Innovation Center of Sustainable Forestry in Southern China of Jiangsu Province, Nanjing Forestry University, Nanjing, China, [2]Department of Microbiology and Plant Biology, University of Oklahoma, Norman, OK, USA, [3]Center for Ecosystem Science and Society, Department of Biological Sciences, Northern Arizona University, Flagstaff, AZ, USA, [4]University of Oklahoma Information Technology, Norman, OK, USA, [5]Environmental Sciences Division and Climate Change Science Institute, Oak Ridge National Laboratory, Oak Ridge, TN, USA, [6]Department of Earth System Science, Tsinghua University, Beijing, China

Key Points:
- Observations from ongoing SPRUCE experiments constrained forecasting of carbon cycles under future warming
- The parameter uncertainty primarily contributes to uncertainty in forecasting C pool-based response variables
- The stochasticity in future external forcing primarily contributes to uncertainty in forecasting C flux-based response variables

Supporting Information:
- Supporting Information S1
- Data Set S1

Correspondence to:
J. Jiang,
ecologyjiang@gmail.com

Citation:
Jiang, J., Huang, Y., Ma, S., Stacy, M., Shi, Z., Ricciuto, D. M., et al. (2018). Forecasting responses of a northern peatland carbon cycle to elevated CO_2 and a gradient of experimental warming. *Journal of Geophysical Research: Biogeosciences*, *123*, 1057–1071. https://doi.org/10.1002/2017JG004040

Received 10 JUL 2017
Accepted 6 MAR 2018
Accepted article online 9 MAR 2018
Published online 25 MAR 2018

Abstract The ability to forecast ecological carbon cycling is imperative to land management in a world where past carbon fluxes are no longer a clear guide in the Anthropocene. However, carbon-flux forecasting has not been practiced routinely like numerical weather prediction. This study explored (1) the relative contributions of model forcing data and parameters to uncertainty in forecasting flux- versus pool-based carbon cycle variables and (2) the time points when temperature and CO_2 treatments may cause statistically detectable differences in those variables. We developed an online forecasting workflow (Ecological Platform for Assimilation of Data (EcoPAD)), which facilitates iterative data-model integration. EcoPAD automates data transfer from sensor networks, data assimilation, and ecological forecasting. We used the Spruce and Peatland Responses Under Changing Experiments data collected from 2011 to 2014 to constrain the parameters in the Terrestrial Ecosystem Model, forecast carbon cycle responses to elevated CO_2 and a gradient of warming from 2015 to 2024, and specify uncertainties in the model output. Our results showed that data assimilation substantially reduces forecasting uncertainties. Interestingly, we found that the stochasticity of future external forcing contributed more to the uncertainty of forecasting future dynamics of C flux-related variables than model parameters. However, the parameter uncertainty primarily contributes to the uncertainty in forecasting C pool-related response variables. Given the uncertainties in forecasting carbon fluxes and pools, our analysis showed that statistically different responses of fast-turnover pools to various CO_2 and warming treatments were observed sooner than slow-turnover pools. Our study has identified the sources of uncertainties in model prediction and thus leads to improve ecological carbon cycling forecasts in the future.

1. Introduction

Forecasting how increasing atmospheric CO_2 and temperature will affect ecosystems in the future is a central topic of global change ecology. An increasing number of climate change manipulative experiments have been initiated to study how ecosystems response to rising CO_2 and/or increasing temperature (Hanson et al., 2016; Luo et al., 2001; Norby et al., 2005; Roy et al., 2016). The knowledge gained from these experiments must be integrated into models to fill the gaps in understanding ecological processes under future climate. In the past, many modeling exercises have been widely used to predict responses of ecosystems to elevated atmospheric CO_2 and global warming (Luo & Reynolds, 1999; Parton et al., 2007). However, large uncertainties in the model predictions hindered our predictive understanding of land ecosystem responses to global change (Cramer et al., 2001; De Kauwe et al., 2014; Sitch et al., 2008). Forecasting ecosystem responses to climate change from a model using a particular set of parameters driven by a certain trajectory of external forcing is uninformative without fully specified uncertainties, because model outputs will differ with minor changes in parameters or external forcings (Dietze, 2017). Few modeling studies have incorporated interactive model-data integration to produce near-time forecasts, especially for ongoing manipulative experiments. However, such integration is vital to the improvement and advancement of carbon cycle forecasting.

The uncertainty of carbon cycle model results stems from three fundamental components upon which all models rely: model structure, parameterization, and external forcings (Luo et al., 2016). Terrestrial carbon

cycle models simplify complex physical and biological processes. Different strategies to incorporate underrepresented processes resulting from simplification could cause model structure uncertainty (Smith et al., 2013; William et al., 2015). Manipulative ecosystem-scale experiments, by investigating ecosystem responses to novel conditions, can provide insights into underrepresented processes. Unfortunately, the addition of more detailed processes to models leads to an increase in forecasting uncertainty because of the increase in the numbers of parameters and equifinality in data assimilation, which can be difficult to constrain (De Kauwe et al., 2017; Luo et al., 2009; Luo, Keenan, & Smith, 2015).

While data assimilation that feeds empirical data into terrestrial carbon models can improve our understanding of parameter uncertainties (Bloom & Williams, 2015; Clark et al., 2001; Dietze, 2014; Hararuk & Luo, 2014; Keenan, Davidson, Moffat, et al., 2012), relative contributions of forcing uncertainty in carbon cycle forecasting are less studied. On one hand, external forcing variables such as temperature, precipitation, and light regulate various aspects of carbon cycle processes (e.g., plant photosynthesis, water use, and soil carbon decomposition) and therefore influence ecosystem carbon pools (Becknell et al., 2015; Medvigy et al., 2010; Seddon et al., 2016). On the other hand, parameters describing the functional properties of ecosystems determine how ecosystems respond to external forcings. A challenge in precisely predicting the future state of an ecosystem is partly due to the difficulty in constraining parameters of complex models and the low predictability of future trajectories of forcing variables. Some studies have used forcing variables from various climate components of general circulation models to drive a specific land model at the global scale (Ahlström et al., 2012, 2013; Berthelot et al., 2005). However, these studies have failed to consider parameter uncertainty. It is clear that different data sets have information to constrain different subset of parameters. For example, eddy flux data can only constrain a few flux-based parameters and need ancillary pool-based data to constrain parameters such as plant carbon allocation and turnover rates (Du et al., 2015; Keenan, Davidson, Munger, et al., 2012; Zhang et al., 2010). Conversely, it is unclear to what extent adding the variation of future forcing trajectories to a constrained model would increase forecasting uncertainty and what response variables are most affected by forcing uncertainty.

Here we apply the model-data fusion approach to a climate change manipulative experiment, the Spruce and Peatland Responses Under Changing Experiments (SPRUCE; Hanson et al., 2016), to investigate the relative contribution of forcing and parameter uncertainties in the forecasting of terrestrial carbon cycles. The decade-long SPRUCE experiment manipulates both deep soil and air temperature to produce whole ecosystem warming treatments. Atmospheric CO_2 is also elevated in half of the manipulated plots to assess ecosystem-level biological responses to atmospheric changes that may realistically coincide with warming in the future. Data assimilation (section 2.2) is used to estimate the posterior distribution of model parameters based on pretreatment data sets (2011–2014) at SPRUCE. Parameter uncertainty was then analyzed by randomly choosing sets of parameters from the posterior distributions. Forcing uncertainty was represented by ensemble trajectories of a 10 year (2015–2024) stochastic weather generator (section 2.3). The decade-long timescale was chosen to match planned experimental period in SPRUCE, which is also a reasonable timescale to test changes of pool-based variables in response to climate change treatments. Using the ensemble of parameters and forcings, we ran many simulations over the range of 2015–2024 for uncertainty analysis under ambient conditions (section 2.4) and forecasted treatment effects under the experimental treatments (section 2.5). In section 2.4, we designed full factorial simulation experiments that quantify uncertainties in forecasting gross primary productivity (GPP), ecosystem respiration (ER), and carbon stocks in foliage, wood, root, and soil pools. We then analyzed the relative contribution of stochasticity in forcings and parameter uncertainties to the uncertainties in forecasting these flux-based and pool-based response variables. In section 2.5, we predicted the responses of the northern peatland ecosystem to atmospheric CO_2 fertilization and a gradient of experimental warming over the next decade in SPRUCE with fully specified uncertainties. We then evaluated how long the experiment would need to be conducted to observe ecosystem changes of different response variables.

2. Method

2.1. Site Description and Operational Forecasting System

The SPRUCE experiment is conducted in a *Picea mariana* (black spruce)-*Sphagnum* spp. ombrotrophic forested peatland located in the USDA Forest Service Marcell Experimental Forest (MEF) in Northern

Minnesota, USA. The site (N47°30.476′, W93°27.162′, 418 m above mean sea level) is a potentially vulnerable ecosystem located in the southern fringes of the extant boreal-peatland range. Significant impacts on peatland carbon cycle dynamics have been hypothesized due to climate change. The historical mean annual air temperature is 3.3°C, with extremes of −46°C (2 February 1996) and 38°C (19 August 1976, 6 July 1988, and 27 July 1988), and the mean annual precipitation is 785 mm (Sebestyen et al., 2011).

The 8.1 ha experimental site (S1-Bog) regenerated from tree removal experiments 40 years ago. The SPRUCE experiment is being operated as the first whole-ecosystem, forest-scale experiment to increase temperature from deep soil to the top of tree canopies and includes exposure to elevated atmospheric CO_2. The design includes 10 plots of 12 m diameter by 8 m high open-top enclosures and two additional designated ambient observation plots. The warming treatments vary from controls (+0°C) to +2.25°C, +4.5°C, +6.75°C, and +9°C. Deep peat heating was initialed in June 2014, and whole-ecosystem warming began in August 2015. Elevated CO_2 (800–900 ppm) was introduced to some plots in June 2016.

The SPRUCE experiment provides a platform to integrate modeling and experimental activities for the benefit of both. Via data assimilation, we translated the variation of pretreatment data into parameter uncertainty. Using historical climate data from a MEF station (Sebestyen et al., 2011), we generated stochastic future trajectories of forcing variables. When new data from the ongoing field campaigns and associated measured environmental data are available, we can update parameter uncertainty and make new projections. To make the workflow interactive and automated, we developed a Web-based application called Ecological Platform for Assimilation of Data (EcoPAD), which is available at http://ecolab.cybercommons.org/ecopad_portal/. All the source code and the Terrestrial ECOsystem Model SPRUCE 1.0 are also available online at https://github.com/ou-ecolab/teco_spruce. Forecasting data are automated and archived monthly in a server located at the University of Oklahoma Supercomputing Center for Education and Research. In this study, we were interested in the relative contribution of parameter and forcing uncertainties to the range of forecasts. Thus, we used EcoPAD to assimilate pretreatment data of 2011–2014 and to forecast carbon dynamics for 2015–2024.

2.2. Data Assimilation

While many studies focus on parameter optimization of complex carbon cycle models containing hundreds of parameters, quantifying fully specified uncertainties of the parameters is not feasible due to computational cost and the lack of multistream data sets. Most data assimilation studies have shown that the number of parameters constrained by observational data is limited, typically from several parameters to less than 20 parameters (Braswell et al., 2005; Xu et al., 2006; Zhou et al., 2015). We used the Terrestrial ECOsystem (TECO) model to predict carbon dynamics in SPRUCE. TECO simulates processes of canopy photosynthesis, plant growth, carbon transfer among pools, and soil water dynamics. The full TECO model has not been used before in data assimilation due to the computational cost. However, an emulator of the TECO model, which can fully reproduce TECO using a matrix approach, has been widely used for data assimilation (Shi et al., 2015; Weng et al., 2011; Xu et al., 2006; Zhou et al., 2010). The photosynthesis module in the full TECO model is represented as input data in the emulator, while carbon transfer among plant and soil pools is modeled in a matrix. External forcing variables were represented by scalars influencing turnover rates of each carbon pool. Using the TECO emulator, Xu et al. (2006) constrained residence times of various plant and soil carbon pools. However, the simplified emulator does not simulate photosynthesis and plant growth. Thus, parameters like specific leaf area (SLA), maximum rate of carboxylation, aboveground and belowground plant growth rates, and growing degree-days cannot be constrained. Here we used the full TECO model to simulate carbon dynamics at SPRUCE, representing a northern peatland.

We compiled 11 pretreatment data sets from 2011 to 2014, three of which included community-scale flux measurements (GPP, NEE, and ER) in 1.2 m internal diameter chambers, six data sets of plant biomass growth and carbon content (foliage, stem, and root), one data set of carbon in peat soil, and leaf phenological data. During 2011–2014, CO_2 flux observations were collected monthly during the growing season at ambient plots in the S1-Bog. A total of 30 data measurements were collected in August, September, and October 2011; May through November 2012; July, September, and October 2013; and June and July 2014 (Hanson et al., 2016). The flux data from pseudo-nighttime observations under a temporary black plastic cover were estimated as ER. Uncovered measurements were used to estimate net ecosystem exchange. More details on the design of collar chamber and measurements can be found in Hanson et al. (2016). NEE is defined as the difference between GPP and ER. Thus, we calculated GPP by summing NEE and ER. We collected three

Table 1
Parameters Involved in Data Assimilation

	Description	Unit	Lower limit	Upper limit	Initial value
V_{cmax}	Maximum rate of carboxylation	$\mu mol\ m^{-2}\ s^{-1}$	14	180	80
τ_{leaf}	Residence time of C in leaf	year	0.5	3.0	1.0
τ_{wood}	Residence time of C in wood	year	5	80	40
τ_{root}	Residence time of C in root	year	0.3	2	0.8
$\tau_{finelitter}$	Residence time of C in fine litter	year	0.1	0.5	0.3
$\tau_{coarselitter}$	Residence time of C in coarse litter	year	1.0	20	5.8
$\tau_{fastSOM}$	Residence time of C in fast turnover soil organic matter	year	0.05	0.8	0.4
$\tau_{slowSOM}$	Residence time of C in slow turnover soil organic matter	year	5	150	50
$\tau_{passiveSOM}$	Residence time of C in passive soil organic matter	year	300	4,000	2,000
$g_{maxleaf}$	Maximum growth rate of foliage	day^{-1}	0.02	0.15	0.1
$g_{maxroot}$	Maximum growth rate of root	day^{-1}	0.02	0.15	0.1
$g_{maxstem}$	Maximum growth rate of stem	day^{-1}	0.02	0.1	0.05
$r_{0\ leaf}$	Baseline respiration of foliage	$\mu mol\ m^{-2}\ s^{-1}$	10	45	30
$r_{0\ root}$	Baseline respiration of root	$\mu mol\ m^{-2}\ s^{-1}$	10	45	30
$r_{0\ stem}$	Baseline respiration of stem	$\mu mol\ m^{-2}\ s^{-1}$	5	10	7
Q_{10}	Sensitivity of respiration to temperature	—	1	3	2
SLA	Specific leaf area	$cm^{-2}\ g^{-1}$	10	200	40
gdd_{onset}	Minimum degree-days for plant leaf out	°C	100	160	140

annual data points from 2012 to 2014 for plant foliage, woody biomass, and aboveground net primary production. Biomass data were compiled by combining allometric data for shrubs (*Ledum*, *Chamaedaphne*, and *Vaccinium*), all ground layer species, and trees (*P. mariana* and *Larix laricina*; Hanson et al., 2012). In the summers of 2012–2014, the plants were harvested from the plots and then processed and measured in areas adjacent to the experimental study plots. Only one data point was collected each for fine-root and peat soil C. Fine-root peak growth and standing crop measurements were collected from root in-growth cores throughout the growing seasons of 2013 (Iversen et al., 2017). Peat carbon was collected from core samples of peat in the SPRUCE experimental plots over the summer of 2011 (Iversen et al., 2014; Wilson et al., 2016). Samples were collected from the hummock and hollow surfaces to depths of 200–300 cm in defined increments. Flowering or leaf-out dates were observed during 2011–2014 (Hanson et al., 2015). We used leaf-out dates for data assimilation, which corresponded to the date growing degree-days above a threshold in the TECO model. The standard deviations reported in these data sets were also compiled to estimate uncertainties for each data stream.

We applied the Bayesian probabilistic inversion approach to estimate the posterior distribution of 18 parameters, representing key ecological processes in the TECO model (Table 1). The maximum rate of carboxylation (V_{cmax}) is widely used to determine leaf-level photosynthesis (Hu et al., 2014, Walker, Beckerman, et al., 2014), which can be rescaled to community-level productivity through leaf area index and SLA. Allocation of primary production to different plant organs is controlled by growth rates and autotrophic respiration of each organ. We picked the maximum growth rates of foliage ($g_{maxleaf}$), root ($g_{maxroot}$), and stem ($g_{maxstem}$) for data assimilation. Autotrophic respirations of different organs were modeled by baseline respirations ($r_{0\ leaf}$, $r_{0\ root}$, $r_{0\ stem}$) and environmental scalars. Carbon contents in each plant and soil pool are sensitive to the residence time (Table 1), which has been widely used for data assimilation in previous studies (Hararuk, Xia, & Luo, 2014; Shi et al., 2015; Weng & Luo, 2011). The prior ranges of residence time in each carbon pool were based on Shi et al. (2015) and Zhou et al. (2010), and prior ranges of maximum growth rates and baseline respiration were based on Weng and Luo (2011) and Zhou, Wan, and Luo (2007). According to the Bayes' theorem, the posterior probability density function $p(\theta|Z)$ of model parameters θ for given observations Z can be obtained from prior probability density function $p(\theta)$ and the likelihood function $p(Z|\theta)$.

$$p(\theta|Z) \propto p(Z|\theta)p(\theta) \quad (1)$$

From prior knowledge, the parameters represented by $p(\theta)$ were assumed uniformly distributed. The likelihood function describes information contained in data sets. Assuming that errors between each

observational data set and model simulation are independently following Gaussian distribution with a zero mean, then the likelihood function can be expressed by

$$p(Z|\theta) \propto \exp\left\{-\sum_{i=1}^{11}\sum_{t\in Z_i}\frac{[Z_i(t)-X(t)]^2}{2\sigma_i^2(t)}\right\} \quad (2)$$

where $Z_i(t)$ is the ith (a total of 11 data sets) observation data set at time t, $X(t)$ is the model simulation outputs for the variables corresponding to observations, and $\sigma_i(t)$ is the standard deviation of each measurement.

Posterior probability distributions of parameters were generated by the Markov chain Monte Carlo sampling technique using the adaptive Metropolis-Hastings algorithm (Figure S1). Specifically, we repeated two steps until generating a converged Markov chain of parameter space. In the first step, we proposed a new vector of parameters θ^{new} based on the previously accepted parameters θ^{old} by a proposal distribution $p(\theta^{\text{new}}|\,\theta^{\text{old}})$. In the second step, the new vector of parameters is tested against the Metropolis criterion to determine whether it should be accepted or not. We adopted the Gaussian distribution to generate θ^{new}:

$$\theta^{\text{new}} = \theta^{\text{old}} + N(0,\ \text{cov}(\theta)) \quad (3)$$

where $N(0, \text{cov}(\theta))$ is the Gaussian distribution with mean of zeros and covariance $\text{cov}(\theta)$ is calculated from previous accepted parameters. We recalculated $\text{cov}(\theta)$ at fixed steps of 500 simulations to update covariance matrix. We run four chains of 50,000 simulations with an acceptance rate between 23% and 44%. The first half of accepted parameters were discarded (burn-in period), and the rest were used to generate posterior parameter distributions. In this study, we applied the Gelman-Rubin diagnostic statistics to examine the convergence of the four chains.

2.3. Stochastic Weather Generation

External forcing of TECO SPRUCE 1.0 includes hourly climate data of photosynthetically active radiation (PAR), air temperature, soil temperature, precipitation, relative humidity, vapor pressure deficit, and wind speed. We took records of 2011–2014 from an environmental monitoring station at S1-Bog for data assimilation. Then, we generated an ensemble of 300 trajectories of 10 year forcing variables from 2015 to 2024 as inputs for the forecasting period. We also obtained historical precipitation and air temperature data from 1961 to 2014 at the USDA MEF station, which represents long-term climate for the S1-Bog. Detailed MEF station information was published by Sebestyen et al. (2011). Precipitation and air temperature were generated by vector autoregression (VAR) using the 1961–2014 data set using the R package RMAWGEN (Pfaff, 2008). Analogous to the autoregressive model, the VAR model fits time series data from its own previous values. The VAR model is also able to capture the covariance among multiple time series. The algorithm allowed us to generate drivers for all the experimental plots in SPRUCE. In this study, we fitted the VAR model to air temperature and precipitation at the MEF station. A pth order VAR model, denoted VAR(p), can be expressed as follows:

$$Y_t = a_0 + A_1 Y_{t-1} + \ldots + A_p Y_{t-p} + B_1 X_{t-1} + \ldots + B_p X_{t-p} + U_t$$

where Y_t is a K-dimensional vector representing the set of weather variables at K plots generated at day t by the model, called "endogenous" variable, X_t is the corresponding K-dimensional vector for other weather variables, called "exogenous" variables, A_i and B_i are $K \times K$ coefficient matrices, and U_t is a K-dimensional stochastic process.

The RMAWGEN package used Akaike information criterion to determine optimal orders. We got an order of 3 for precipitation and an order of 10 for air temperature. We first generated daily precipitation by VAR(3) without exogenous variables and then generated daily mean, minimum, and maximum air temperature by VAR(10) using precipitation as exogenous variables to account for covariance. Both models passed the normality test and seriality test, which verify the absence of time autocorrelation of the VAR residuals. To further generate hourly data, we simply divided the daily precipitation by 24 to get precipitation data in each hour of a day (Waichler & Wigmosta, 2003). Waichler and Wigmosta (2003) compared a uniform distribution and a relative fraction based method that fractions of rainfall in each hour were derived from monthly average. They found no significant difference between the two methods with little diurnal pattern in precipitation. Hourly air temperature was interpolated from minimum and maximum daily temperatures by R package

Table 2
Factorial Design of Simulation Experiments Resulted From Parameter and Forcing Uncertainties

External forcings were drawn from	Parameters were drawn from	Uncertainty sequence number	Ensemble group number
Ensemble of forcing variables	Prior distribution	1	1
	Posterior distribution	2	2
	Fixed at certain values	3	2
Fixed at certain trajectories	Prior distribution	4	1
	Posterior distribution	5	2
	Fixed at certain values	6	—

Note. The uncertainty sequence numbers were corresponding to bar numbers in Figure 4. Two groups of simulation ensemble were distinguished by drawing parameters from prior or posterior distributions.

Interpol.T (Eccel, 2010). The package estimates hourly temperature using a sine function from the minimum temperature at sunrise until the maximum temperature is reached, another sine function from the maximum temperature until sunset, and a square root function from then until sunrise the next morning (Cesaraccio et al., 2001).

Three of the meteorological drivers, PAR, relative humidity, and wind speed, were coupled and randomly drawn from frequency distributions at a given hour each month. Specifically, we constructed a 24 (hours) by 12 (months) matrix field. Within each field, a coupled pool of the three drivers was obtained from S1-Bog climate data during 2011–2014. We then generated PAR, relative humidity, and wind speed for 2015–2024 by resampling the set of drivers from the pools. Soil temperature at 20 cm depth was scaled from the generated air temperature based on a linear regression between soil temperature and air temperature at S1-Bog from 2011 to 2014. Vapor pressure deficit was calculated from the difference between the saturation vapor pressure and actual partial pressure of the water vapor in the air, which was computed by multiplying relative humidity with the saturation vapor pressure.

The algorithm decoupled PAR, relative humidity, and wind speed from temperature and precipitation, which might generate biased covariance among the meteorological drivers at hourly timescale. To examine whether the biased covariance would influence forecasting uncertainty, we generated other trajectories of meteorological drivers by simply resampling from the 2011–2014 data sets at the S1-Bog. Specifically, meteorological drivers for 2015 were resampled from one of the years from 2011 to 2014, and then we repeated resampling until 2024. In this case, the covariance among meteorological drives from generated time series would be the same as the covariance from the actual 2011–2014 time series.

2.4. Uncertainty Analysis

We designed a full factorial simulation experiment to disentangle the relative contribution of forcing and parameter uncertainties to the forecasting uncertainty. We set up three levels of parameter uncertainties: prior uniform distribution, posterior distribution, and a given set of constrained parameters. We also set up two levels of forcing uncertainties: stochastic forcing from an ensemble, and predefined, fixed trajectories of forcing. Thus, we produced a total of six levels of uncertainties (Table 2). Forecasting uncertainty was quantified by standard deviation at the year 2024 for two flux variables (GPP and ER) and four pool size variables (foliage, wood, root, and soil). Since TECO model is deterministic, forecasting uncertainties are zero when parameters were fixed at certain values and forcing variables were fixed at certain trajectories. We normalized the uncertainties to make sure forecasting uncertainty equals one when parameters were randomly drawn from a prior distribution and forcing trajectories were picked from the ensemble of stochastic weather generator.

Based on the full factorial design, we produced two groups of simulation ensemble with each group consisting of 2,500 simulations (Table 2). To get the first ensemble of simulation group, we randomly chose 50 sets of parameters within the prior ranges and 50 trajectories from an ensemble of future forcings, which resulted in a combination of 2,500 model simulations. We then calculated standard deviation at the year 2024 for the six response variables as forecasting uncertainties resulted from prior parameters and stochastic forcings. The other ensemble of 2,500 simulations resulted from 50 sets of posterior parameters and the same

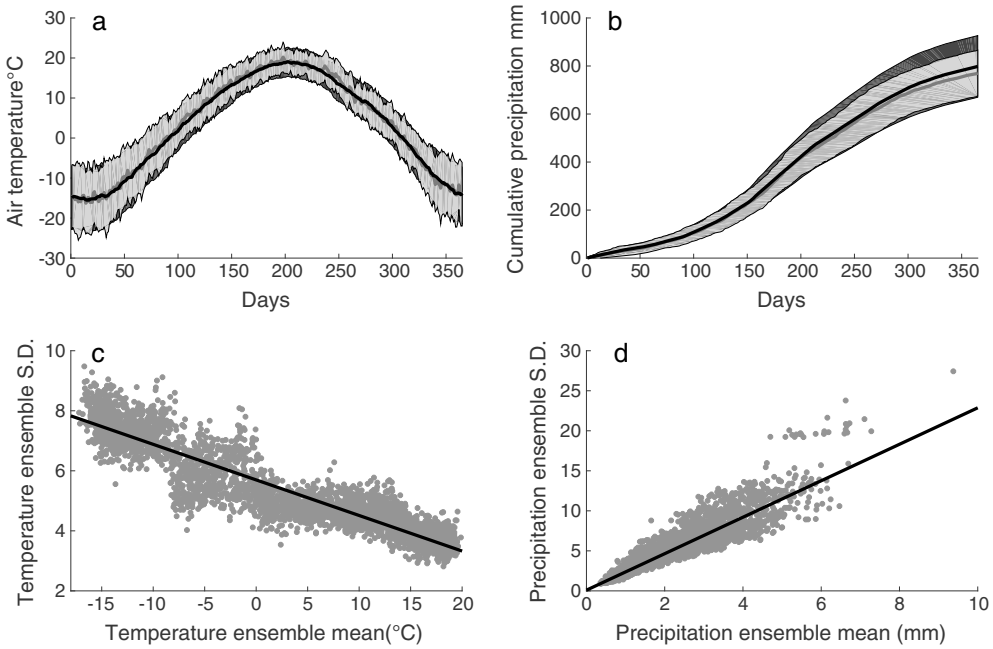

Figure 1. Historical climate from the USDA MEF site during 1961–2014 and stochastic weather generation for 2015–2024. (a) Daily air temperature and (b) cumulative precipitation along Julian calendar. Curves and shaded areas represent mean and standard deviation (S.D.), respectively (gray is historical data, and black areas represent ensemble of future data). (c) and (d) are standard deviations of ensembles against means of each day for air temperature and precipitation, respectively.

consistent 50 trajectories of stochastic forcings used in the first group. Forecasting uncertainties caused by stochastic forcings alone can be estimated from a subgroup of simulations using the 50 trajectories of forcings under a given set of parameters. We calculated 50 uncertainties from the stochastic forcings alone for each of the 50 fixed parameters from the second ensemble group. The standard deviation of the 50 uncertainties represented the sensitivity of forcing caused by the uncertainty of parameters (error bars of uncertainties). Similarly, we used the first and second ensemble group to calculate 50 uncertainties for each of the 50 fixed forcing trajectories from prior parameters alone and from posterior parameters alone, respectively. Sensitivities of parameter caused by uncertainties in forcing variables were evaluated from the standard deviation of the normalized uncertainties. The last uncertainty level is zero as expected from deterministic model simulations for a given set of fixed parameters and a given trajectory of forcing.

2.5. Forecasting Treatment Effects

After the parameter and forcing uncertainties were fully specified at the ambient environment for the SPRUCE site, we ran forecasting simulations for the 10 SPRUCE treatments (five levels of elevated temperature with two levels of elevated atmospheric CO_2). Each scenario contains 300 simulations with sets of coupled parameters randomly chosen from accepted parameters by data assimilation and the forcing trajectories from the stochastic weather generator. We assumed that all treatments started the first day of 2015, although actual start dates of treatment varied, and that the parameters estimated from pretreatment data did not change during the forecasting period or among treatments. The assumption was probably unrealistic but provided a basis for understanding future states based on current information. When more data sets are available, our EcoPAD platform will provide real-time forecasting and demonstrate how parameters evolve. Based on pretreatment data, we estimated how long the experiment takes to observe the differences among the 10 experimental treatments. We did one-way ANOVA tests and Tukey's multiple comparisons for each of the pool-based response variables (foliage, wood, root, and soil) for each of the 10 scenarios. The tests were iterated daily from 1 January 2015 to the end of 2024. We recorded the first dates that the response variables for each scenario became significantly different from the other scenarios and that remained significantly

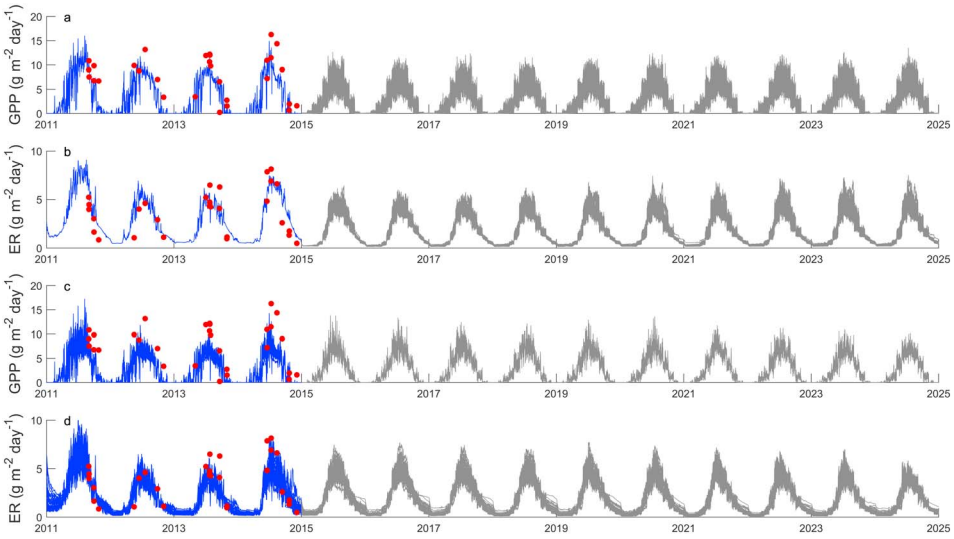

Figure 2. Projections of GPP and ER during 2011–2024. In (a) and (b), parameters were fixed while forcing variables were drawn from stochastic trajectories. In (c) and (d), parameters were drawn from posterior distribution while the trajectory of forcing variables was given. The period 2011–2014 was the model training period (blue) with data points (red) from field measurement. The period 2015–2024 is the forecasting period (gray).

different for the remainder of the period. The time between 1 January 2015 and the identified dates were then reported as the period needed for the treatment to become statistically different from other treatments.

3. Results

3.1. Uncertainty in Precipitation and Temperature

Using the VAR model, our generated precipitation and air temperature during 2015–2024 matched the overall probability distributions of historical data during 1961–2014 with low interannual variability (Figures 1a and 1b). Annual mean temperature from 1961 to 2014 was 3.4°C and 2.6–3.7°C for the ensemble generated for 2015–2024. Annual precipitation from weather generator occurred mainly during the summer with slightly higher variation than the variability of historical observations. The stochasticity of the weather generator resulted in the uncertainty of forcing variables. The standard deviation of temperature ensemble decreases with increasing daily mean temperature (Figure 1c), which implies higher uncertainty of future temperature in winter than that in summer. The standard deviation of precipitation ensemble increases with increasing daily rainfall (Figure 1d). With higher precipitation in summer than in winter at the MEF station, Figure 1d implies that uncertainty of future precipitation is higher in summer than in winter.

3.2. Sources of Forecasting Uncertainty

Forecasting uncertainties due to uncertainties in parameters or forcings were quite different between flux-based and pool-based response variables. External forcings resulted in higher variation than parameters in forecasting GPP and ER (Figure 2) but lower variation than parameters in forecasting carbon stock in foliage, wood, root, and soil (Figure 3). Forecasting of carbon fluxes had lower interannual variability than simulations from 2011 to 2014 (Figure 2).

The factorial analysis of sources of uncertainty in forecasting showed higher uncertainties when parameters were unconstrained and external forcing trajectories were stochastic (Figure 4). If the parameters were constrained by data assimilation, uncertainties in forecasting the response variables were reduced, regardless of whether the external forcing trajectories were stochastic (compare bar 1 and bar 2) or fixed (compare bar 4 and bar 5). Nevertheless, further fixing the parameter values cannot further reduce uncertainties in forecasting GPP and ER (compare bar 2 and bar 3). Fixing parameter values could further reduce uncertainty in forecasting pool-based variables. If all the parameters were randomly drawn from prior ranges, improving forcing predictability did not reduce uncertainties in forecasting pool-based carbon but did considerably reduce GPP uncertainty (compare bar 1 and bar 4). The normalized uncertainty indices in Figure 4 showed

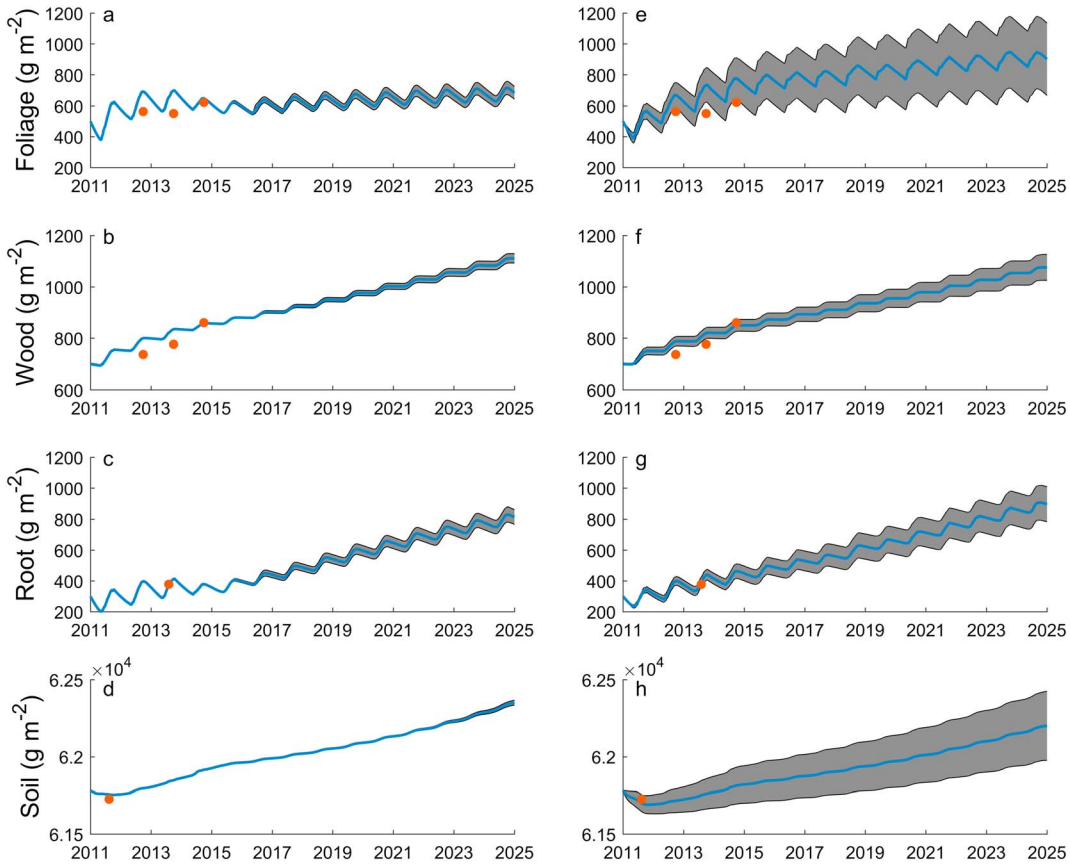

Figure 3. Uncertainties in forecasted carbon pools from forcing variables and parameter values. Mean (blue line) and standard deviation (shaded area) of foliage, wood, root, and soil carbon during 2011–2024 as influenced by stochastic forcing variables (a–d) and parameter uncertainties (e–h). The period 2011–2014 is the model training period with data points (red) from field measurements, and 2015–2024 is the forecasting period.

that uncertainty of GPP and ER in year 2024 caused by forcing alone was higher than the parameter alone, but uncertainty of foliage, wood, root, and soil in the year 2024 caused by forcing alone were lower than the parameter alone (compare bar 3 to bar 5). Using the resampled meteorological drivers from 2011 to 2014 data sets, the forecasting uncertainties associated with forcings were reduced,

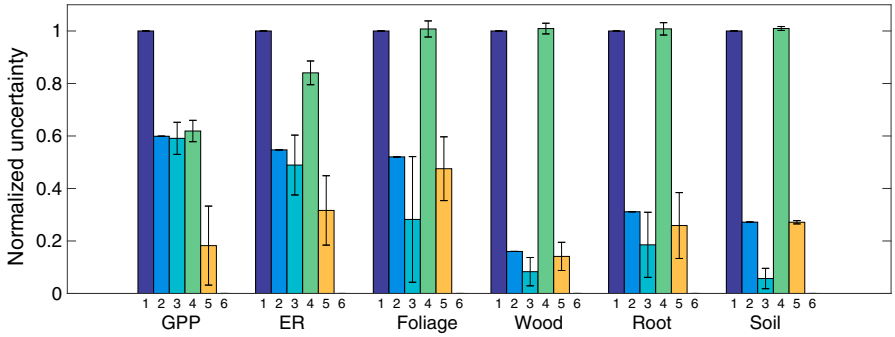

Figure 4. Factorial uncertainty analysis of flux-based (GPP and ER) and pool-based (foliage, wood, root and soil) response variables caused by six combinations of forcing and parameter uncertainty levels: (1) prior parameters and stochastic forcings, (2) posterior parameters and stochastic forcings, (3) stochastic forcings alone, (4) prior parameters alone, (5) posterior parameters alone, and (6) fixed parameters and a specific trajectory of forcing. Error bars represent standard deviation of normalized uncertainty when available. Bar 6 was zero, and bar 1 was normalized to 1.

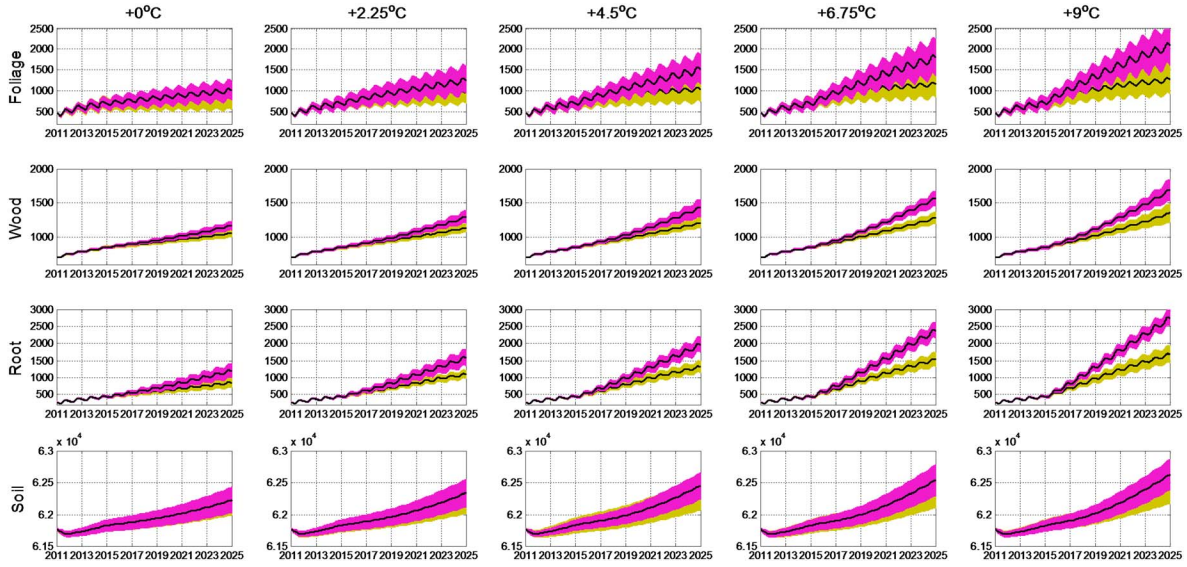

Figure 5. Projections of foliage, wood, root, and soil carbon under warming and elevated atmospheric CO_2 treatments. Shaded areas above or below the curves were one standard deviation away from mean trajectories for ambient (yellow) and elevated (purple) CO_2.

especially the uncertainty of ER caused by forcing alone was reduced greatly and lower than the parameter alone (Figure S2).

3.3. Forecasting Treatment Effects With Fully Specified Uncertainties

Both warming and elevated CO_2 increased carbon stock in foliage, wood, root, and soil, but uncertainty in forecasting reduced the statistical power to detect the treatment effects (Figure 5). Plant compartments had stronger responses to either warming or elevated CO_2 than soil carbon. Differences of response between ambient and elevated CO_2 were more likely significant at higher temperature treatments (Figure 6). For example, the foliage difference between ambient and elevated CO_2 did not become significant until the end of experimental period (9.5 years) without warming but only took 1.5 years with temperature treatments of +6.75°C and +9°C (Figure 6A). While soil carbon needs 6 years to respond to elevated CO_2 at +9°C treatment, it did not respond to elevated CO_2 at low-temperature treatments during the entire experimental period (Figure 6D). Wood and root had faster responses than foliage and soil (Figures 6B and 6C). Responses to warming treatments took longer under ambient CO_2 than elevated CO_2 (Figure 6). Particularly, the foliage difference between +0°C and +2.25°C was not significant during the experimental period under ambient CO_2 but only took 1.7 years under elevated CO_2 (Figure 6A).

4. Discussion

Northern peatland ecosystems are vulnerable to future climate change and are expected to change over the course of this century. But forecasting how northern peatland ecosystems respond to global warming and elevated CO_2 tends to differ across models. Model-experiment integration has been proposed to reduce the uncertainty (Luo et al., 2009, 2012; Norby & Luo, 2004). It is common for modelers to tune models to fit data from a specific experiment (De Kauwe et al., 2014; Luo, Ogle, & Tucker, 2011). Those tuned models, which often overlook intrinsic uncertainties of parameters and external forcings, have a low predictive ability in other sites (Li et al., 2016). We developed a novel framework, the EcoPAD, to fully specify uncertainties when forecasting the responses of an ecosystem to elevated CO_2 and five levels of experimental warming treatment at the SPRUCE experimental site. We found that external forcing produced higher uncertainties than parameters in the forecasting of C flux-based response variables but lower uncertainties than parameterization in forecasting C pool-based response variables.

The contrasting contribution of external forcing and parameterization in the uncertainty of forecasting between C flux-based and C pool-based response variables was probably related to timescales of different

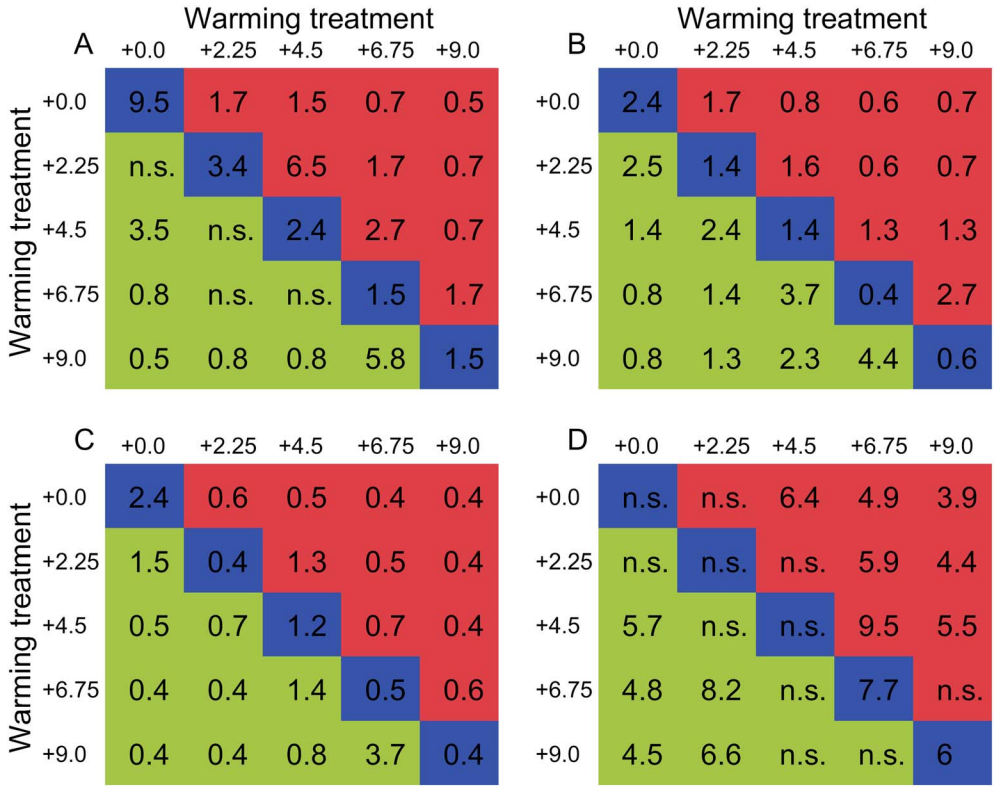

Figure 6. Delayed responses of (a) foliage, (b) wood, (c) root, and (d) soil carbon to the treatments. The numbers are how many years since 1 January 2015 that it took for the responses to become significantly different for each pair. The values were presented as a matrix for each pair of temperature levels underlying rows and columns. The red pixels represent warming treatment under elevated CO_2. The green pixels represent warming treatment alone under ambient CO_2. The blue pixels bisecting the matrix represent treatment of elevated CO_2 under each temperature level. n.s. is not significant for that pair of comparison within the 10 year simulations.

ecological processes and their sensitivity to external forcing. Photosynthesis is highly sensitive to light, temperature, and moisture, which may fluctuate widely over minute timescale. Changes of sunlight and precipitation have great influences on terrestrial ecosystem carbon dynamics (Medvigy et al., 2010). Predictive ability of the C flux-based response variables, in this case, is largely determined by the precision of forcing prediction. In some pseudo-forecasting exercises, the model projection of C fluxes fit observed values very well, if external forcing is already known (Feng & Dietze, 2013; Keenan, Davidson, Moffat, et al., 2012; Oikawa et al., 2017). Therefore, in predictive carbon cycle science, when forecasting C fluxes such as NEE by eddy flux or ecosystem respiration using the static chamber, the research community should consider the uncertainty in external forcings. The weather generator algorithms used in this study may not be able to capture realistic trajectories, but our study was not intended to improve predictability of hourly meteorological drivers. We used the weather generator to generate an ensemble of future meteorological drivers with predefined uncertain levels, which allows us to distinguish relative contribution of external forcing and parameter uncertainty in forecasting uncertainties. We found that uncertainty in future external forcing contributed more to uncertainty in the forecasting of C flux-based response variables than is the parameter uncertainty. The conclusion was consistent in forecasting pool-based response variables despite biased covariance among meteorological drivers in our weather generator algorithm. However, preserved driver covariance could reduce the uncertainties of flux-based response variables. The results should stimulate the research communities' efforts in predictive carbon science to improve the predictability of future forcing when forecasting C flux-based response variables. Over the last several decades, the accuracy of 5 day weather forecasts has increased from 60% to 90% (Bauer et al., 2015). Although weather forecasting has improved for short timescales ranging from hours to days, it is still unreliable at longer timescales (Bauer et al., 2015). Therefore, it is anticipated that forecasting of C

flux-based response variables could be substantially improved on short-time prediction, for example, weekly, before weather forecasting can be done over longer time or downscaling of climate prediction can be accurately performed.

Uncertainty in forecasting C pool-based response variables mainly stemmed from parameterization instead of external forcing. This is probably because the pool change is cumulative. Instantaneous changes in forcing variables were smoothed over time while parameters that determine carbon allocation and turnover directly control the accumulation rates. Parameters that influence pool sizes vary among species and across space and time (Johnson et al., 2016; Mc Cormack et al., 2014; Thurner et al., 2016). The pool-based pretreatment data sets were scarce at the SPRUCE site with only one observation for soil and root C, three observations of foliage and wood, which may have resulted in relatively high uncertainty of pool-based parameters. Among the parameters that affect residence times and growth rates, only foliage and root residence time were constrained (Figure S1). Third, both GPP and ER are sensitive to forcings, for example, temperature, in the same direction, which may result in balanced input and output to ecosystem carbon stock. From a meta-analysis of Free-Air CO_2 Enrichment (FACE) experiments, van Groenigen et al. (2014) found that soil C pool was not sensitive to elevated CO_2 because both net primary production and soil decomposition increased with CO_2. C pool-based response variables may be sensitive to extreme events and future climate change (Frank et al., 2015; Reichstein et al., 2013). Our stochastically generated weather has low interannual variability. This low variability is likely due to the ensemble of forcing trajectories generated by our algorithm, which used averages for the past four decades. Algorithms that generate more realistic interannual variability are needed for future studies.

Model structure is also a major source of forecasting uncertainty although it was not evaluated in this study. By comparing experimental responses with scenario simulations among models, one can evaluate the main assumptions causing differences and reduce uncertainty in model structure (Medlyn et al., 2015). For example, data from ecosystem-scale FACE experiments were compared to 11 process-based models and found out that models with net primary production allocation among different plant organ varies with elevated CO_2 can perform better than constant allocation models (De Kauwe et al., 2014; Medlyn et al., 2015; Walker, Hanson, et al., 2014). By assimilating data from SPRUCE experiment periodically, our workflow facilitates iterative data-model integration and can identify which parameters will change with treatments and how fast the changes would be. Thus, it can help us to improve mechanistic understanding of northern peatland ecosystem responses to increases in temperature and exposures to elevated atmospheric CO_2. But before the experimental results are fully available to evaluate model structure, uncertainties in parameterization and external forcing should be clearly identified, because two different models could produce similar results if the models are tuned to match data and therefore bias the evaluation of model structure. Our data assimilation platform, by assimilating multiple streams of data set into models, could provide fully specified uncertainties on how a model behaves with a range of forecasting instead of single tuned model output. We suggest that future model comparisons should consider uncertainties of each model.

Our scenario-based simulations reveal that C pool-based response variables are sensitive to warming and CO_2 fertilization. Time points to observe statistical difference among treatments also vary in different response variables. For example, differences in statistical biomass among warming treatments were not apparent until the third year in an open-top chamber experiment of grassland (Carlyle et al., 2014). Twenty years of warming on a moist acidic tussock tundra ecosystem increased plant carbon storage but did not change total soil carbon (Sistla et al., 2013). A meta-analysis indicated that both plant part C and microbial biomass C were not statistically changed in response to warming in those 5–10 year manipulative experiments but became statistically different in $>$10 year warming (Lu et al., 2013). Increasing soil respiration and litter mass loss can be observed in a short duration of warming experiments (Lu et al., 2013; Rustad et al., 2001). However, warming did not significantly alter the SOC pool in most experiments (Lu et al., 2013). One major reason is that enhanced litter decomposition and soil respiration offsets the warming-induced increase in plant-derived C influx. Our results suggest that changes in SOC might be detectable in manipulative experiments with longer duration and higher warming magnitude.

Reducing the forecasting uncertainty could increase the statistical power to detect the treatment effects. The greater contribution to uncertainty by parameters than drivers in forecasting pool-based variables implies that constraining the parameters via data assimilation could cause the forecasted treatment effects to

occur sooner than unconstrained parameters. Our projections were based on pretreatment data and assumed that the plant community did not change with warming and elevated CO_2. However, several studies found that the plant community may change with long-term warming, which can influence carbon cycles with nonlinear responses (Xu et al., 2015). For example, warming increased plant diversity at Cedar Creek Ecosystem Science Reserve in Minnesota and caused a greater increase in aboveground productivity (Cowles et al., 2016). An ecosystem may also respond to treatments differently at different successional states (Norby et al., 2016). Thus, the expectation on how long it would take for experimental effects to be observed may be different from real observations. Our EcoPAD platform can update parameters regularly as new data sets become available and reveal when model simulations depart from experimental observations (Huang et al., 2017; Ma et al., 2017).

Acknowledgments
We thank Russell Doughty for language editing. This work is supported by the National Natural Science Foundation of China (41701225, 41601209), National Key R&D Program of China (2017YFC0505502), Jiangsu Province Science Foundation for Youths (BK20170920), subcontract 4000144122 from the Oak Ridge National Laboratory (ORNL) to the University of Oklahoma, and by the Jiangsu Specially-Appointed Professors Program, the priority academic program development of Jiangsu higher education institutions (PAPD). We thank the Northern Research Station of the USDA Forest Service for using the four-decade climate data. All data sets from this study are available on github repository at https://github.com/ou-ecolab/teco_spruce.

References

Ahlström, A., Schurgers, G., Arneth, A., & Smith, B. (2012). Robustness and uncertainty in terrestrial ecosystem carbon response to CMIP5 climate change projections. *Environmental Research Letters*, *7*, 044008.

Ahlström, A., Smith, B., Lindström, J., Rummukainen, M., & Uvo, C. B. (2013). GCM characteristics explain the majority of uncertainty in projected 21st century terrestrial ecosystem carbon balance. *Biogeosciences*, *10*, 1517–1528.

Bauer, P., Thorpe, A., & Brunet, G. (2015). The quiet revolution of numerical weather prediction. *Nature*, *525*, 47–55.

Becknell, J. M., Desai, A. R., Dietze, M. C., Schultz, C. A., Starr, G., Duffy, P. A., et al. (2015). Assessing interactions among changing climate, management, and disturbance in forests: A macrosystems approach. *Bioscience*, *65*(3), 263–274. https://doi.org/10.1093/biosci/biu234

Berthelot, M., Friedlingstein, P., Ciais, P., Dufresne, J.-L., & Monfray, P. (2005). How uncertainties in future climate change predictions translate into future terrestrial carbon fluxes. *Global Change Biology*, *11*, 959–970.

Bloom, A. A., & Williams, M. (2015). Constraining ecosystem carbon dynamics in a data-limited world: Integrating ecological "common sense" in a model–data fusion framework. *Biogeosciences*, *12*, 1299–1315.

Braswell, B. H., Sacks, W. J., Linder, E., & Schimel, D. S. (2005). Estimating diurnal to annual ecosystem parameters by synthesis of a carbon flux model with eddy covariance net ecosystem exchange observations. *Global Change Biology*, *11*, 335–355.

Carlyle, C. N., Fraser, L. H., & Turkington, R. (2014). Response of grassland biomass production to simulated climate change and clipping along an elevation gradient. *Oecologia*, *174*, 1065–1073.

Cesaraccio, C., Spano, D., Duce, P., & Snyder, R. L. (2001). An improved model for determining degree-day values from daily temperature data. *International Journal of Biometeorology*, *45*, 161–169.

Clark, J. S., Carpenter, S. R., Barber, M., Collins, S., Dobson, A., Foley, J. A., et al. (2001). Ecological forecasts: An emerging imperative. *Science*, *293*(5530), 657–660. https://doi.org/10.1126/science.293.5530.657

Cowles, J. M., Wragg, P. D., Wright, A. J., Powers, J. S., & Tilman, D. (2016). Shifting grassland plant community structure drives positive interactive effects of warming and diversity on aboveground net primary productivity. *Global Change Biology*, *22*, 741–749.

Cramer, W., Bondeau, A., Woodward, F. I., Prentice, I. C., Betts, R. A., Brovkin, V., et al. (2001). Global response of terrestrial ecosystem structure and function to CO_2 and climate change: Results from six dynamic global vegetation models. *Global Change Biology*, *7*(4), 357–373. https://doi.org/10.1046/j.1365-2486.2001.00383.x

De Kauwe, M. G., Medlyn, B. E., Walker, A. P., Zaehle, S., Asao, S., Guenet, B., et al. (2017). Challenging terrestrial biosphere models with data from the long-term multi-factor Prairie Heating and CO_2 Enrichment experiment. *Global Change Biology*, *23*(9), 3623–3645. https://doi.org/10.1111/gcb.13643

De Kauwe, M. G., Medlyn, B. E., Zaehle, S., Walker, A. P., Dietze, M. C., Wang, Y.-P., et al. (2014). Where does the carbon go? A model–data intercomparison of vegetation carbon allocation and turnover processes at two temperate forest free-air CO_2 enrichment sites. *New Phytologist*, *203*(3), 883–899. https://doi.org/10.1111/nph.12847

Dietze, M. (2014). Gaps in knowledge and data driving uncertainty in models of photosynthesis. *Photosynthesis Research*, *119*, 3–14.

Dietze, M. C. (2017). Prediction in ecology: A first-principles framework. *Ecological Applications*, *27*, 2048–2060.

Du, Z., Nie, Y., He, Y., Yu, G., Wang, H., & Zhou, X. (2015). Complementarity of flux- and biometric-based data to constrain parameters in a terrestrial carbon model. *Tellus Series B: Chemical and Physical Meteorology*, *67*. https://doi.org/10.3402/tellusb.v67.24102

Eccel, E. (2010). What we can ask to hourly temperature recording. Part II: Hourly interpolation of temperatures for climatology and modelling. *Italian Journal of Agrometeorology*, *15*, 45–50.

Feng, X., & Dietze, M. (2013). Scale dependence in the effects of leaf ecophysiological traits on photosynthesis: Bayesian parameterization of photosynthesis models. *New Phytologist*, *200*, 1132–1144.

Frank, D., Reichstein, M., Bahn, M., Thonicke, K., Frank, D., Mahecha, M. D., et al. (2015). Effects of climate extremes on the terrestrial carbon cycle: Concepts, processes and potential future impacts. *Global Change Biology*, *21*(8), 2861–2880. https://doi.org/10.1111/gcb.12916

Hanson, P. J., Brice, D., Garten, C. T., Hook, L. A., Phillips, J., & Todd, D. E. (2012). *SPRUCE S1 Bog vegetation allometric and biomass data: 2010–2011*. Oak Ridge, TN: Carbon Dioxide Information Analysis Center, Oak Ridge National Laboratory, U.S. Department of Energy. https://doi.org/10.3334/CDIAC/spruce.004

Hanson, P. J., Gill, A. L., Xu, X., Phillips, J. R., Weston, D. J., Kolka, R. K., et al. (2016). Intermediate-scale community-level flux of CO_2 and CH_4 in a Minnesota peatland: Putting the SPRUCE project in a global context. *Biogeochemistry*, *129*(3), 255–272. https://doi.org/10.1007/s10533-016-0230-8

Hanson, P. J., Riggs, J. S., Hook, L. A., & Nettles, W. R. (2015). *SPRUCE S1-Bog phenology movies, 2010–2015*. Oak Ridge, TN: Carbon Dioxide Information Analysis Center, Oak Ridge National Laboratory, U.S. Department of Energy. https://doi.org/10.3334/CDIAC/spruce.011

Hararuk, O., & Luo, Y. (2014). Improvement of global litter turnover rate predictions using a Bayesian MCMC approach. *Ecosphere*, *5*, 1–13.

Hararuk, O., Xia, J., & Luo, Y. (2014). Evaluation and improvement of a global land model against soil carbon data using a Bayesian Markov chain Monte Carlo method. *Journal of Geophysical Research: Biogeosciences*, *119*, 403–417. https://doi.org/10.1002/2013JG002535

Hu, S., Mo, X., & Lin, Z. (2014). Optimizing the photosynthetic parameter V_{cmax} by assimilating MODIS-fPAR and MODIS-NDVI with a process-based ecosystem model. *Agricultural and Forest Meteorology*, *198-199*, 320–334.

Huang, Y., Jiang, J., Ma, S., Ricciuto, D., Hanson, P. J., & Luo, Y. (2017). Soil thermal dynamics, snow cover, and frozen depth under five temperature treatments in an mobrotrophic bog: Constrained forecast with data assimilation. *Journal of Geophysical Research: Biogeosciences*, *122*, 2046–2063. https://doi.org/10.1002/2016JG003725

Iversen, C. M., Childs, J., Norby, R. J., Garrett, A., Martin, A., Spence, J., et al. (2017). *SPRUCE S1 bog fine-root production and standing crop assessed with minirhizotrons in the southern and northern ends of the S1 Bog*. Oak Ridge, TN: Carbon Dioxide Information Analysis Center, Oak Ridge National Laboratory, U.S. Department of Energy. https://doi.org/10.3334/CDIAC/spruce.019

Iversen, C. M., Hanson, P. J., Brice, D. J., Phillips, J. R., Mcfarlane, K. J., Hobbie, E. A., & Kolka, R. K. (2014). *SPRUCE peat physical and chemical characteristics from experimental plot cores, 2012*. Oak Ridge, TN: Carbon Dioxide Information Analysis Center, Oak Ridge National Laboratory, U.S. Department of Energy. https://doi.org/10.3334/CDIAC/spruce.005

Johnson, M. O., Galbraith, D., Gloor, M., de Deurwaerder, H., Guimberteau, M., Rammig, A., et al. (2016). Variation in stem mortality rates determines patterns of above-ground biomass in Amazonian forests: Implications for dynamic global vegetation models. *Global Change Biology*, *22*(12), 3996–4013. https://doi.org/10.1111/gcb.13315

Keenan, T. F., Davidson, E., Moffat, A. M., Munger, W., & Richardson, A. D. (2012). Using model-data fusion to interpret past trends, and quantify uncertainties in future projections, of terrestrial ecosystem carbon cycling. *Global Change Biology*, *18*, 2555–2569.

Keenan, T. F., Davidson, E. A., Munger, J. W., & Richardson, A. D. (2012). Rate my data: Quantifying the value of ecological data for the development of models of the terrestrial carbon cycle. *Ecological Applications*, *23*, 273–286.

Li, Q., Xia, J., Shi, Z., Huang, K., Du, Z., Lin, G., & Luo, Y. (2016). Variation of parameters in a flux-based ecosystem model across 12 sites of terrestrial ecosystems in the conterminous USA. *Ecological Modelling*, *336*, 57–69.

Lu, M., Zhou, X., Yang, Q., Li, H., Luo, Y., Fang, C., et al. (2013). Responses of ecosystem carbon cycle to experimental warming: A meta-analysis. *Ecology*, *94*(3), 726–738. https://doi.org/10.1890/12-0279.1

Luo, Y., Ahlström, A., Allison, S. D., Batjes, N. H., Brovkin, V., Carvalhais, N., et al. (2016). Toward more realistic projections of soil carbon dynamics by Earth system models. *Global Biogeochemical Cycles*, *30*, 40–56. https://doi.org/10.1002/2015GB005239

Luo, Y., Keenan, T. F., & Smith, M. (2015). Predictability of the terrestrial carbon cycle. *Global Change Biology*, *21*, 1737–1751.

Luo, Y., Ogle, K., Tucker, C., Fei, S., Gao, C., La Deau, S., et al. (2011). Ecological forecasting and data assimilation in a data-rich era. *Ecological Applications*, *21*(5), 1429–1442. https://doi.org/10.1890/09-1275.1

Luo, Y., Randerson, J. T., Abramowitz, G., Bacour, C., Blyth, E., Carvalhais, N., et al. (2012). A framework for benchmarking land models. *Biogeosciences*, *9*(10), 3857–3874. https://doi.org/10.5194/bg-9-3857-2012

Luo, Y., & Reynolds, J. F. (1999). Validity of extrapolating field CO_2 experiments to predict carbon sequestration in natural ecosystems. *Ecology*, *80*, 1568–1583.

Luo, Y., Wan, S., Hui, D., & Wallace, L. L. (2001). Acclimatization of soil respiration to warming in a tall grass prairie. *Nature*, *413*, 622–625.

Luo, Y., Weng, E., Wu, X., Gao, C., Zhou, X., & Zhang, L. (2009). Parameter identifiability, constraint, and equifinality in data assimilation with ecosystem models. *Ecological Applications*, *19*, 571–574.

Ma, S., Jiang, J., Huang, Y., Shi, Z., Wilson, R. M., Ricciuto, D., et al. (2017). Data-constrained projections of methane fluxes in a northern Minnesota peatland in response to elevated CO_2 and warming. *Journal of Geophysical Research: Biogeosciences*, *122*, 2841–2861. https://doi.org/10.1002/2017JG003932

Mc Cormack, M. L., Adams, T. S., Smithwick, E. H., & Eissenstat, D. M. (2014). Variability in root production, phenology, and turnover rate among 12 temperate tree species. *Ecology*, *95*, 2224–2235.

Medlyn, B. E., Zaehle, S., De Kauwe, M. G., Walker, A. P., Dietze, M. C., Hanson, P. J., et al. (2015). Using ecosystem experiments to improve vegetation models. *Nature Climate Change*, *5*(6), 528–534. https://doi.org/10.1038/nclimate2621

Medvigy, D., Wofsy, S. C., Munger, J. W., & Moorcroft, P. R. (2010). Responses of terrestrial ecosystems and carbon budgets to current and future environmental variability. *Proceedings of the National Academy of Sciences*, *107*, 8275–8280.

Norby, R. J., De Kauwe, M. G., Domingues, T. F., Duursma, R. A., Ellsworth, D. S., Goll, D. S., et al. (2016). Model–data synthesis for the next generation of forest Free-Air CO_2 Enrichment (FACE) experiments. *New Phytologist*, *209*(1), 17–28. https://doi.org/10.1111/nph.13593

Norby, R. J., Delucia, E. H., Gielen, B., Calfapietra, C., Giardina, C. P., King, J. S., et al. (2005). Forest response to elevated CO_2 is conserved across a broad range of productivity. *Proceedings of the National Academy of Sciences of the United States of America*, *102*(50), 18,052–18,056. https://doi.org/10.1073/pnas.0509478102

Norby, R. J., & Luo, Y. (2004). Evaluating ecosystem responses to rising atmospheric CO_2 and global warming in a multi-factor world. *New Phytologist*, *162*, 281–293.

Oikawa, P. Y., Jenerette, G. D., Knox, S. H., Sturtevant, C., Verfaillie, J., Dronova, I., et al. (2017). Evaluation of a hierarchy of models reveals importance of substrate limitation for predicting carbon dioxide and methane exchange in restored wetlands. *Journal of Geophysical Research: Biogeosciences*, *122*, 145–167. https://doi.org/10.1002/2016JG003438

Parton, W. J., Morgan, J. A., Wang, G., & del Grosso, S. (2007). Projected ecosystem impact of the Prairie Heating and CO_2 Enrichment experiment. *New Phytologist*, *174*(4), 823–834. https://doi.org/10.1111/j.1469-8137.2007.02052.x

Pfaff, B. (2008). VAR, SVAR and SVEC models: Implementation within R package vars. *Journal of Statistical Software*, *27*, 1–32.

Reichstein, M., Bahn, M., Ciais, P., Frank, D., Mahecha, M. D., Seneviratne, S. I., et al. (2013). Climate extremes and the carbon cycle. *Nature*, *500*(7462), 287–295. https://doi.org/10.1038/nature12350

Roy, J., Picon-Cochard, C., Augusti, A., Benot, M. L., Thiery, L., Darsonville, O., et al. (2016). Elevated CO_2 maintains grassland net carbon uptake under a future heat and drought extreme. *Proceedings of the National Academy of Sciences of the United States of America*, *113*(22), 6224–6229. https://doi.org/10.1073/pnas.1524527113

Rustad, L., Campbell, J., Marion, G., Norby, R., Mitchell, M., Hartley, A., et al. (2001). A meta-analysis of the response of soil respiration, net nitrogen mineralization, and aboveground plant growth to experimental ecosystem warming. *Oecologia*, *126*(4), 543–562. https://doi.org/10.1007/s004420000544

Sebestyen, S., Dorrance, C., Olson, D., Verry, E., Kolka, R., Elling, A., & Kyllander, R. (2011). Long-term monitoring sites and trends at the Marcell Experimental Forest. In R. K. Kolka, et al. (Eds.), *Peatland biogeochemistry and watershed hydrology at the Marcell Experimental Forest* (pp. 15–71). New York: CRC Press.

Seddon, A. W. R., Macias-Fauria, M., Long, P. R., Benz, D., & Willis, K. J. (2016). Sensitivity of global terrestrial ecosystems to climate variability. *Nature*, *531*, 229–232.

Shi, Z., Xu, X., Hararuk, O., Jiang, L., Xia, J., Liang, J., et al. (2015). Experimental warming altered rates of carbon processes, allocation, and carbon storage in a tallgrass prairie. *Ecosphere*, *6*, 1–16.

Sistla, S. A., Moore, J. C., Simpson, R. T., Gough, L., Shaver, G. R., & Schimel, J. P. (2013). Long-term warming restructures Arctic tundra without changing net soil carbon storage. *Nature*, *497*, 615–618.

Sitch, S., Huntingford, C., Gedney, N., Levy, P. E., Lomas, M., Piao, S. L., et al. (2008). Evaluation of the terrestrial carbon cycle, future plant geography and climate-carbon cycle feedbacks using five Dynamic Global Vegetation Models (DGVMs). *Global Change Biology*, *14*(9), 2015–2039. https://doi.org/10.1111/j.1365-2486.2008.01626.x

Smith, M. J., Purves, D. W., Vanderwel, M. C., Lyutsarev, V., & Emmott, S. (2013). The climate dependence of the terrestrial carbon cycle, including parameter and structural uncertainties. *Biogeosciences*, *10*, 583–606.

Thurner, M., Beer, C., Carvalhais, N., Forkel, M., Santoro, M., Tum, M., & Schmullius, C. (2016). Large-scale variation in boreal and temperate forest carbon turnover rate related to climate. *Geophysical Research Letters*, *43*, 4576–4585. https://doi.org/10.1002/2016GL068794

van Groenigen, K. J., Qi, X., Osenberg, C. W., Luo, Y., & Hungate, B. A. (2014). Faster decomposition under increased atmospheric CO_2 limits soil carbon storage. *Science*, *344*, 508–509.

Waichler, S. R., & Wigmosta, M. S. (2003). Development of hourly meteorological values from daily data and significance to hydrological modeling at H. J. Andrews Experimental Forest. *Journal of Hydrometeorology*, *4*, 251–263.

Walker, A. P., Beckerman, A. P., Gu, L., Kattge, J., Cernusak, L. A., Domingues, T. F., et al. (2014). The relationship of leaf photosynthetic traits – *V*(cmax) and *J*(max) – to leaf nitrogen, leaf phosphorus, and specific leaf area: A meta-analysis and modeling study. *Ecology and Evolution*, *4*(16), 3218–3235. https://doi.org/10.1002/ece3.1173

Walker, A. P., Hanson, P. J., De Kauwe, M. G., Medlyn, B. E., Zaehle, S., Asao, S., et al. (2014). Comprehensive ecosystem model-data synthesis using multiple data sets at two temperate forest free-air CO_2 enrichment experiments: Model performance at ambient CO_2 concentration. *Journal of Geophysical Research: Biogeosciences*, *119*, 937–964. https://doi.org/10.1002/2013JG002553

Weng, E., & Luo, Y. (2011). Relative information contributions of model vs. data to short- and long-term forecasts of forest carbon dynamics. *Ecological Applications*, *21*, 1490–1505.

Weng, E., Luo, Y., Gao, C., & Oren, R. (2011). Uncertainty analysis of forest carbon sink forecast with varying measurement errors: A data assimilation approach. *Journal of Plant Ecology*, *4*, 178–191.

William, R. W., Cory, C. C., David, M. L., & Gordon, B. B. (2015). Effects of model structural uncertainty on carbon cycle projections: Biological nitrogen fixation as a case study. *Environmental Research Letters*, *10*, 044016.

Wilson, R. M., Hopple, A. M., Tfaily, M. M., Sebestyen, S. D., Schadt, C. W., Pfeifer-Meister, L., et al. (2016). Stability of peatland carbon to rising temperatures. *Nature Communications*, *7*, 13723. https://doi.org/10.1038/ncomms13723

Xu, T., White, L., Hui, D., & Luo, Y. (2006). Probabilistic inversion of a terrestrial ecosystem model: Analysis of uncertainty in parameter estimation and model prediction. *Global Biogeochemical Cycles*, *20*, GB2007. https://doi.org/10.1029/2005GB002468

Xu, X., Shi, Z., Li, D., Zhou, X., Sherry, R. A., & Luo, Y. (2015). Plant community structure regulates responses of prairie soil respiration to decadal experimental warming. *Global Change Biology*, *21*, 3846–3853.

Zhang, L., Luo, Y., Yu, G., & Zhang, L. (2010). Estimated carbon residence times in three forest ecosystems of eastern China: Applications of probabilistic inversion. *Journal of Geophysical Research*, *115*, G01010. https://doi.org/10.1029/2009JG001004

Zhou, T., Shi, P., Jia, G., Dai, Y., Zhao, X., Shangguan, W., et al. (2015). Age-dependent forest carbon sink: Estimation via inverse modeling. *Journal of Geophysical Research: Biogeosciences*, *120*, 2473–2492. https://doi.org/10.1002/2015JG002943

Zhou, X., Luo, Y., Gao, C., Verburg, P. S. J., Arnone, J. A., Darrouzet-Nardi, A., & Schimel, D. S. (2010). Concurrent and lagged impacts of an anomalously warm year on autotrophic and heterotrophic components of soil respiration: A deconvolution analysis. *New Phytologist*, *187*, 184–198.

Zhou, X., Wan, S., & Luo, Y. (2007). Source components and interannual variability of soil CO_2 efflux under experimental warming and clipping in a grassland ecosystem. *Global Change Biology*, *13*, 761–775.